Steel and Composite Structures, Vol. 10, No. 1 (2010) 1-21
DOI: http://dx.doi.org/10.12989/scs.2010.10.1.001

Experimental and numerical investigations into the composite behaviour of steel frames and precast concrete infill panels with window openings

P.A. Teeuwen*, C.S. Kleinman, H.H. Snijder and H. Hofmeyer

Eindhoven University of Technology, Eindhoven, the Netherlands

(Received September 11, 2008, Accepted February 6, 2009)

Abstract. As an alternative for conventional structures for tall buildings, a hybrid lateral load resisting structure has been designed, enabling the assembly of tall buildings directly from a truck. It consists of steel frames with discretely connected precast concrete infill panels provided with window openings. Besides the stiffening and strengthening effect of the infill panels on the frame structure, economical benefits may be derived from saving costs on materials and labour, and from reducing construction time. In order to develop design rules for this type of structure, the hybrid infilled frame has recently been subjected to experimental and numerical analyses. Ten full-scale tests were performed on one-storey, one-bay, 3 by 3 m infilled frame structures, having different window opening geometries. Subsequently, the response of the full-scale experiments was simulated with the finite element program DIANA. The finite element simulations were performed taking into account non-linear material characteristics and geometrical non-linearity. The experiments show that discretely connected precast concrete panels provided with a window opening, can significantly improve the performance of steel frames. A comparison between the full-scale experiments and simulations shows that the finite element models enable simulating the elastic and plastic behaviour of the hybrid infilled frame.

Keywords: infilled frame; steel; precast concrete; lateral resistance; experiments; finite element analysis.

1. Introduction

Construction time, more than ever, is a cost-crucial factor. Reducing construction time means saving money both directly and indirectly, for example due to reduced hindrance to the surroundings of the building site. Reduction of construction time can be achieved by many means, for example by the use of prefabricated elements, dry connections or more intelligent construction procedures. Meeting the demand of reduced construction time, a hybrid lateral load resisting structure has been designed for the construction of tall buildings at Eindhoven University of Technology. The structure consists of infilled steel frames with discretely connected precast concrete infill panels, enabling the assembly of tall buildings directly from a truck. Besides the stiffening and strengthening effect of the infill panels on the frame structure, economical benefits may be derived from saving costs on materials and labour, and from reducing construction time.

The use of precast concrete panels in steel frames is a new area of application in infilled frames,

* Corresponding Author, E-mail: p.a.teeuwen@upcmail.nl

although the phenomenon of 'infilled frame' has a long history. Since the early fifties extensive investigations have been carried out into the structural behaviour of framed structures with masonry and cast-in-place concrete infills (Holmes 1961, Ng'andu 2006). When connectors or strong bonding at the interfaces between the frame and the infill panel are absent as for example with masonry infill, the structures are known in the literature as non-integral infilled frames (Fig. 1(a)). When these structures are subjected to lateral loading, a large portion of the load is taken up by the infill panel at its loaded corner. The provision of strong bonding or connectors at the interface enables the two components (frame and panel) to act compositely. These infilled frames are known as fully-integral infilled frames (Fig. 1(b)). Part of the shearing load is transmitted from the frame to the infill panel through the connectors. Because of the stiffening and strengthening effect of infill panels on frames, the sway of the structure under lateral loading is considerably reduced. Even with window openings in the infill panels, the lateral stiffness of a framed structure can significantly be improved (Mallick and Garg 1971, Liauw 1972).

In the past decades several methods have been suggested by various investigators for the analysis of infilled frames. The simplest and most highly developed method is based on the concept of equivalent diagonal strut, as initially proposed by Polyakov (1957), and later developed by other investigators (Holmes 1961, Stafford Smith 1962, 1966 and Mainstone 1971). In this method, the infilled frame structure is modelled as an equivalent braced frame system with a compression diagonal replacing the infill. The main challenge of this approach is to determine the width of the diagonal strut, which is related to the relative stiffness of the frame against the infill. Since the diagonal strut concept was not suitable to predict the ultimate strength of a structure, plastic design principles were proposed to estimate the ultimate lateral load resistance of infilled frames (Wood 1978) and Liauw and Kwan 1983). The formulation was based on the principle of virtual work which, alas, was not suitable to evaluate the stiffness of a structure. The development of finite element methods offered some relief to the shortcomings pointed out above. Since the first effort to model infilled frames with finite elements by Mallick and Severn (1967), the finite element method has been extensively used in both static and dynamic analyses of infilled frames.

Preceding research (Tang, *et al*. 2000, Hoenderkamp, *et al*. 2005, Teeuwen, *et al*. 2008a, 2008b) has shown that precast concrete infill panels may be able to achieve at least similar improvements in structural performance to masonry and cast-in-place concrete infills. Infilled frames with discrete connections between frame and panel are denoted as semi-integral infilled frames (Fig. 1(c)). By completely different structural behaviour due to the application of discrete frame-to-panel connections, existing theories for non-integral and fully-integral infilled frames are not suitable for analysing semi-integral infilled frames. New design rules are needed to facilitate the application of this lateral load resisting system for the construction of (tall) buildings. This research project aims at developing these design rules.

In order to develop design rules, the infilled frame structure is currently subjected to experimental, numerical and theoretical analyses. To provide insight into the behaviour of this structure, full-scale experiments on one-storey one-bay infilled frame structures were carried out. To be able to evaluate more thoroughly any stresses and deformations in the structure, the experiments were supplemented by finite element analyses. This article describes the experimental and numerical research that was carried out, and discusses the results. Finally, important conclusions considering the hybrid infilled frame behaviour are given.

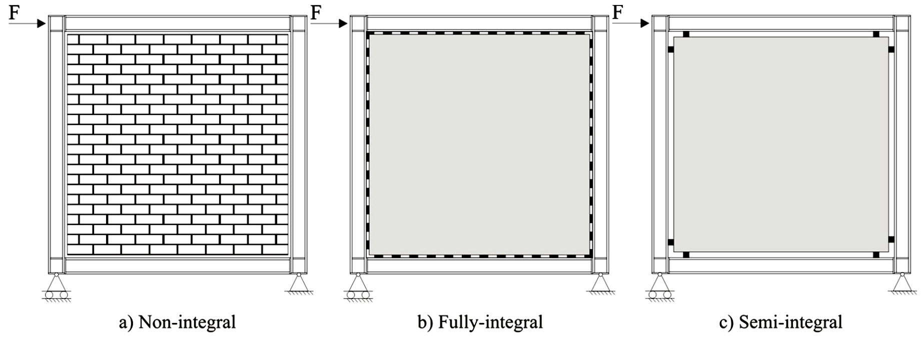

Fig. 1 Classification of infilled frames

2. Discrete interface connection

A discrete frame-to-panel connection has been developed, enabling steel frames and precast concrete panels to act compositely when subject to lateral loading. It is realized by structural bolts on the column and beam in every corner of the steel frame, confining the precast concrete infill panel within the steel frame (Fig. 2) leaving a (50 mm) gap between steel and concrete along the complete panel circumference.

When the infilled frame is loaded laterally, the lateral load is transferred from the frame to the panel through the bolts. Due to a relative low transverse stiffness of the bolts in relation to their axial stiffness, the bolts are mainly loaded in compression. Through the fact that the connections are unable to transfer tensile forces, only the bolts in the compressive corners are active in the laterally loaded system. Consequently, the infill panel has to act as a diagonal strut under compression. Fig. 3 presents the accompanying strut-and-tie model giving the load distribution in the panel by a truss mechanism. The global effect of the infill panel is analogous to the action of a compression diagonal. Therefore, the overall infilled frame behaviour can be compared to an equivalent braced frame system with a compression diagonal replacing the infill panel (see Fig. 3).

To introduce forces into the infill panel, steel angle members are cast at every corner of the panel. To prevent high stress concentrations in the angle members directly under the compression bolts, high-strength steel caps are applied there. The infilled frame structure is designed to fail by a bolt failure

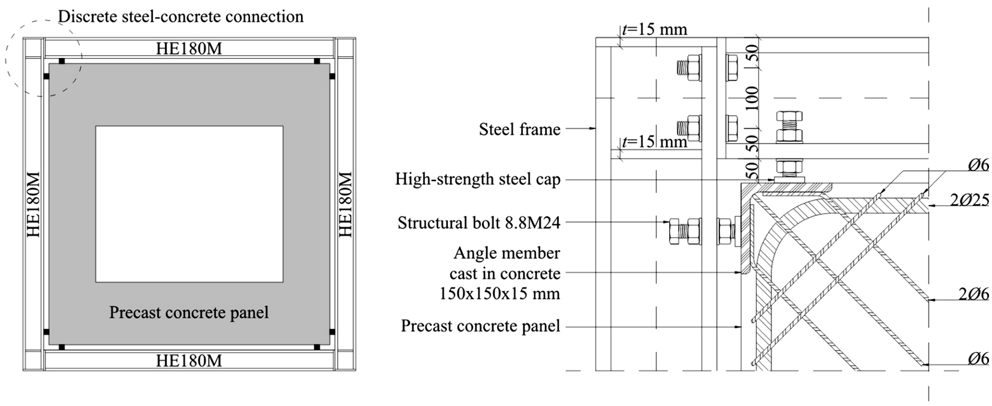

Fig. 2 Infilled steel frame with precast concrete infill panel

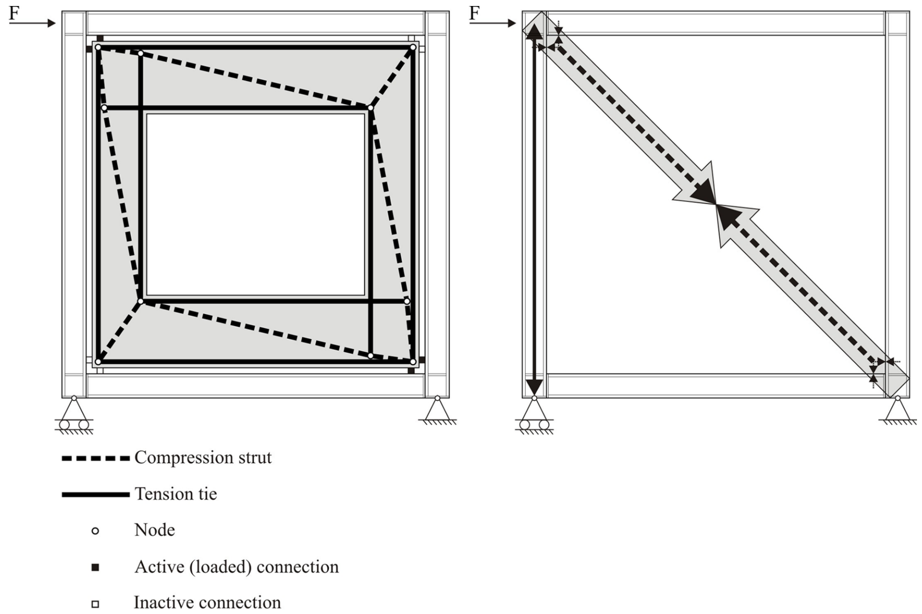

Fig. 3 Load distribution in laterally loaded infilled frame and equivalent braced frame representation

mechanism. Failure of the bolts will not directly result in failure of the entire structure, as force transmission will still occur in the loaded corners of the frame by contact pressure between frame and panel (fail safe concept). Moreover, bolts can easily be replaced while the steel structure and the concrete panel remain undamaged. The anticipated failure mode is shearing of the bolt through the nut. To provide insight into this failure behaviour, preceding investigations into the structural behaviour of the different components of the steel-concrete connection were carried out (Teeuwen, *et al*. 2007). This investigation showed that the bolts subject to axial compressive loading fail by thread stripping failure and not by yielding of the bolt as in the case of bolts subject to tensile loading.

The connection is a dry connection which will function immediately after assembly. Besides, the connections are able to adopt tolerances and enable exact positioning of the panels in both horizontal and vertical direction.

3. Full-scale experiments

3.1 Objectives of experiments

In order to provide insight into the composite behaviour between steel frames and discretely connected precast concrete infill panels provided with a window opening, full-scale experiments on one-storey one-bay infilled frame structures were conducted. The main objectives of the full-scale experiments were to observe the general behaviour of the structures in terms of stiffness, strength and ductility. At the same time, the influence of the chosen parameter, being the size and position of the window opening, was investigated. Besides, the results of these experiments were used to validate a finite element model that will be used to carry out parametric studies.

3.2 Test specimens

The one-storey, one-bay, 3 by 3 m infilled frame structure subject to lateral loading consists of a simply connected steel frame, constructed of HE180M sections in S235 for columns and beams. The discrete frame-to-panel connections, designed for a 'bolt failure' mechanism, were constructed with comparatively weak 8.8 bolts with grade 8 nuts in combination with the heavy flanges of HE180M members. Results obtained from numerical simulations with a FE-model for flanges in bending (Teeuwen, *et al*. 2007) showed that no plastic deformation of the flanges is to be expected for this section. Also for this reason it was decided that a single steel frames could be used for several experiments. Therefore, two identical steel frames were used for the 10 full-scale tests. To investigate the effect of the size and position of the window opening in the infill panel on the infilled frame behaviour, five different panel geometries were tested (Fig. 4). Each panel was tested twice (once in each direction), resulting in a total number of 10 full-scale tests. The five precast reinforced concrete panels ($l \times h \times t = 2700 \times 2700 \times 200\ \mathrm{mm}^3$) were alternately discretely connected to one of the steel frames.

The design of the main bending reinforcement was performed using the strut-and-tie method. The "standard method" of the shear design procedure that can be found in Eurocode 2 was used to design the members of the concrete panel to resist shear. Based on the results of these methods, the panels were all reinforced with longitudinal reinforcement Ø25 and stirrup reinforcement Ø8 with a concrete cover of 15 mm. Angle members (150 × 150 × 15) in S235 were cast in every corner of the panel. Wedge reinforcement was provided in the corners to prevent concrete tensile splitting there. All applied

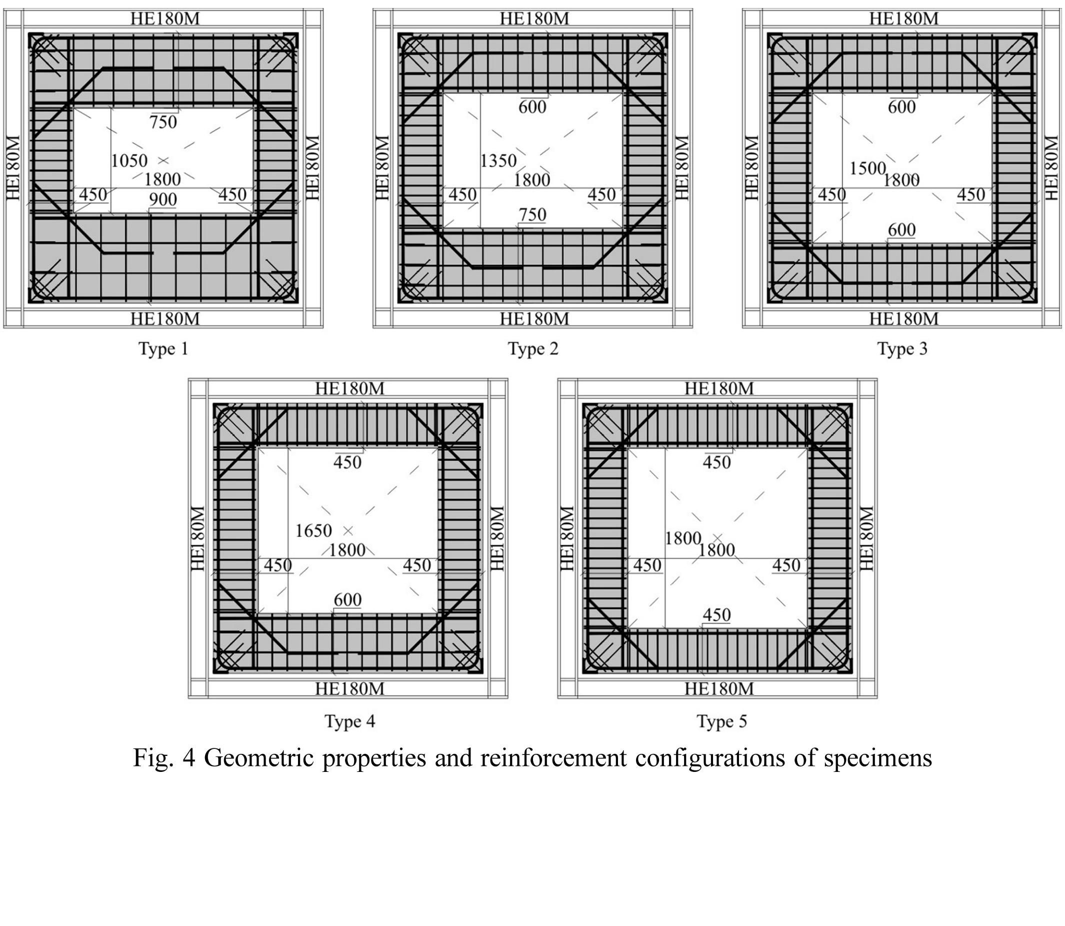

Fig. 4 Geometric properties and reinforcement configurations of specimens

reinforcement was FeB500. The panels were cast in a precast-concrete factory. A self-compacting concrete was applied of concrete grade C45/55. The concrete mixture comprises aggregates (sand (0 - 6 mm) and gravel (4 - 16 mm)), limestone meal, Portland cement CEM I 52,5 R (which develops a high early strength that is needed for a one-day casting cycle), super plasticizer, and water (water-cement ratio = 0.45).

3.3 Test setup

A specifically designed test rig was used to perform the full scale tests on the infilled frame structures (Fig. 5(a)). This test rig is composed of two rigid triangular frames, constructed of HE300B members. These two triangular frames are linked through rigid steel members at their corners. A specimen can be positioned between the two triangular frames and is supported on two different supports. At the side of the jack, the lower corner of the specimen is fixed in the vertical direction to the test rig by four steel M30 rods (Support A, Fig. 5(c)). This support is intended to act as a roller support with a restrained displacement in vertical direction only. At the opposite lower corner, the specimen is supported in a heavy steel block which restrains the specimen from both horizontal and vertical displacement (Support

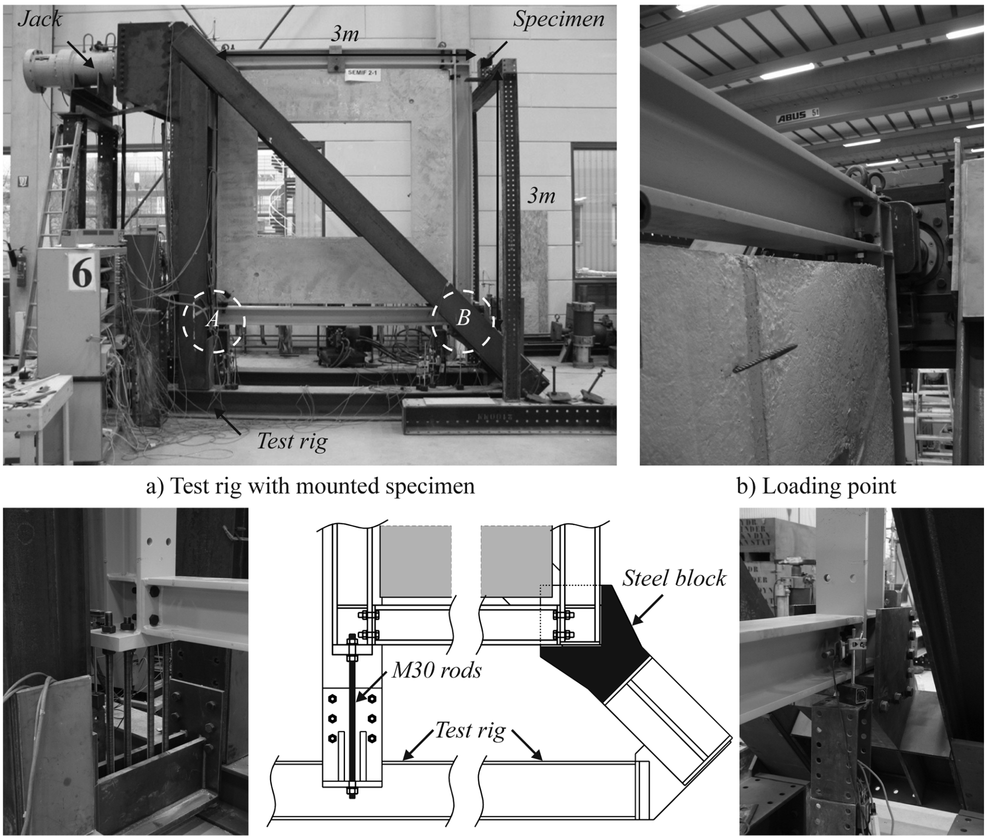

a) Test rig with mounted specimen

b) Loading point

c) Support A

d) Support B

Fig. 5 Test setup

B, Fig. 5(d)). This support is supposed to act as a pin support. A specimen can be loaded laterally by a hydraulic jack that is coupled to the top corner of the triangular frames by stiff steel plates, acting at the height of the top beam centre (Fig. 5(b)). This jack has a stroke of 200 mm and a capacity of 2 MN.

3.4 Measurements

The specimens were instrumented with Linear Variable Differential Transformers (LVDTs) to measure global displacements at the four corners of both frame ($\Delta 1$ to $\Delta 8$) and panel ($\Delta 9$ to $\Delta 16$), deformations of the discrete frame-to-panel connection ($\delta 1$ to $\delta 12$) and panel deformations ($\delta 13$ and $\delta 14$). To find the strain distribution in the precast concrete panel, strain gauge rosettes (gauge lengths 60 mm) were placed on specific locations (Rosettes A to K) on one side of the specimen. These locations are situated in the centre of the compression struts, and on nodes between these struts. Measurements in the tension zones of the panel were made with 6 LVDTs (δa to δf) over a distance of 300 mm. A scheme of arrangement of the instrumentation is shown in Fig. 6. During the tests, story deflections and the lateral loads were monitored. Newly initiated cracks and crack propagation were marked on the specimens and failure mechanisms were observed.

3.5 Testing procedures

In order to quantify the contribution of an infill panel to the stiffness of its confining frame structure, the stiffness of the bare frame structure (without the infill) has to be known. For that reason, the bare frame was tested each time before mounting the precast concrete infill panel within the frame. Therefore, first the beams and columns were assembled. The bolts in the beam-to-column connections were torque controlled tightened up to a specified torque of 400 Nm, to obtain identical initial stiffnesses of the bare frames for all tests as best possible. Other conditions that might influence the coefficient of friction and so the torque as e.g. surface conditions, corrosion and temperature, are supposed to remain

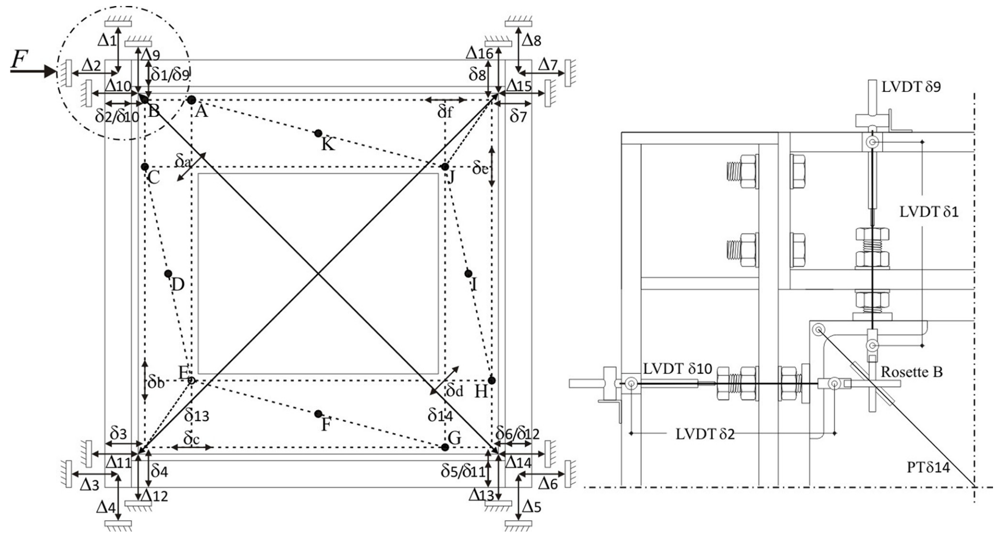

Fig. 6 Measurement scheme

unchanged as each time the same series of bolts were used within identical climatic circumstances. The test procedure of the bare frames involved a preload up to 20 kN to close up initial gaps and contact tolerances between the specimen and the test rig. After the unloading, the bare frames were loaded again up to a load of 60 kN. This load was chosen such, that deformations of the frame would be in the elastic range and therefore did not influence the infilled frame behaviour.

After the bare frame was tested, it was fixed to the horizontally positioned panel. Then, the discrete connection bolts were placed and tightened up to a specified torque of 275 Nm, once again to provide identical boundary conditions as best possible for all tests. Since the infilled-frames were assembled in a horizontal position, the dead weight did not influence the initial prestress levels in the bolts. After erecting the infilled frame structure and thereupon installing the measurement instrumentation, it was positioned in the test rig. The testing procedure of the infilled frames involved a preload of 50 kN (and unloading), for reasons stated earlier. Next, the infilled frames were loaded up to failure. For both bare frame and infilled frame, the load was applied under controlled displacement conditions. For this purpose the stroke of the jack was controlled at 1 mm/min. At this rate, the duration of the tests with the infilled frames was about 1 hour.

As mentioned before, all panels were tested a second time. To this end, the panel was turned around its vertical axis of symmetry and replaced in the confining frame. By doing this, the tension zones where cracks had developed during the first test with the panel became compression zones during the second test, causing the cracks to close. The possible effect of the initially present cracks on the global structural behaviour was investigated by making measurements on the panels. Again, the bare frame structure was tested before the panel was mounted.

Finally, after the last infilled frame test had been carried out, one bare frame was loaded up to failure in order to provide additionally insight into the non-linear behaviour of the bare frame.

4. Experimental observations and results

The most relevant results to describe the major full-scale behaviour characteristics and to verify the finite element model are briefly summarized in this section. A more thorough survey of the test results can be found in Teeuwen, *et al.* (2008).

Fig. 7 presents the load-deflection response of the most far deflected bare frame. Up to a lateral deflection of 35 mm, the response can be reasonably accurately approximated by a graph consisting of two linear branches with an initial ($k_{ini;bf}$) and tangent stiffness ($k_{tan;bf}$). Thereafter, the stiffness decreases due to plastic deformations occurring in the beam-to-column connection. Values for $k_{ini;bf}$ and $k_{tan;bf}$ are in the order of 5.1 and 2.5 kN/mm respectively. Actual bare frame stiffnesses for each bare frame test are shown in Table 1. On the basis of these results, the rotational spring stiffnesses of the beam-to-column connections can be determined, which will be used for the calibration of the finite element models.

In Fig. 8 the load-deflection response of the 10 tested infilled frames and the bare frame considered above is shown. The second number in the test code refers to the first or second test respectively with the same panel. The graphs show the actual deflection of the specimens, which means that a correction has been made for rigid body displacements and rotations. These occur as a result of deformations of the test rig and sliding of the specimen in its supports, and have to be deducted from the total measured deflection to obtain the actual deflection of the specimens only. In order to determine the actual lateral deflection of each specimen, the displacement measured at the loaded upper corner of the specimen

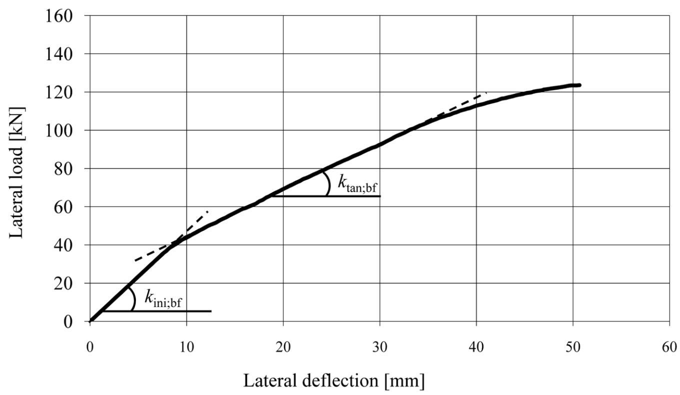

Fig. 7 Load-deflection response of bare frame

Table 1 Test results

Spec. type	Test No.	Stiffness [kN/mm]						Strength [kN]	Failure location*
		Bare frame		Infilled frame					
		$k_{\text{ini;bf}}$	$k_{\text{tan;bf}}$	$k_{\text{sec;1;if}}$	$k_{\text{sec;2;if}}$	$k_{\text{tan;if}}$	α	F_{u}	
1	1-1	5.1	2.5	43.5	21.5	29.8	11.9	701	δ10
	1-2	5.2	2.4	46.1	31.7	32.0	13.3	650	δ11
2	2-1	5.4	2.4	36.9	24.2	27.6	11.5	684	δ10
	2-2	5.4	2.8	38.2	26.8	25.3	9.0	658	δ11
3	3-1	5.8	2.1	33.9	15.9	22.6	10.8	719	δ12
	3-2	4.7	2.4	28.0	18.4	19.3	8.0	719	δ12
4	4-1	4.6	2.4	33.2	18.4	20.3	8.5	656	δ10
	4-2	4.9	2.6	28.7	18.5	20.7	8.0	704	δ12
5	5-1	5.2	2.5	25.1	15.0	16.1	6.4	664	(Panel)
	5-2	4.8	2.6	20.1	12.5	10.3	4.0	583	(Panel)

* For locations, see Fig. 6

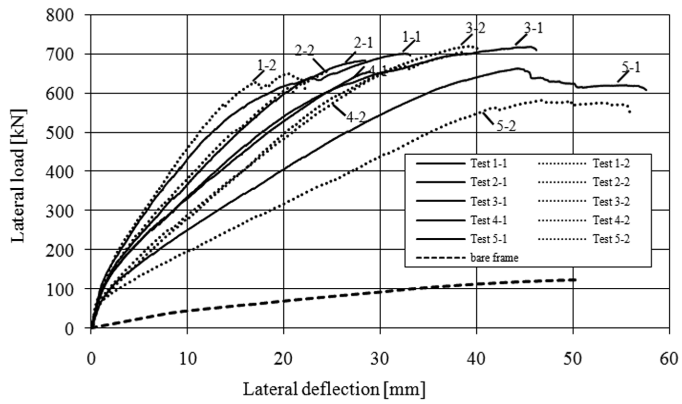

Fig. 8 Load-deflection response of infilled frames

($\Delta 2$) was reduced by the displacements due to rigid body translation and rotation measured at the specimen corners by LVDTs $\Delta 4$, $\Delta 5$ and $\Delta 6$ (for the measurement scheme, see Fig. 6).

The typical infilled frame behaviour is characterised by a relatively high initial stiffness, resulting from the tightening and thus prestressing of the discrete frame-to-panel connections in combination with uncracked panel behaviour. Next, the lateral stiffness decreases due to crack initiation and can be considered linear up to around 500 kN, followed by a non-linear branch and finally failure. For test numbers 1-1 to 4-2, failure of the infilled frame structures occurred by shearing of the frame-to-panel connection bolts through the nuts by stripping of the threads of the bolts (Fig. 9). Although the differences between the normal force levels in the bolts are only marginal, the bolts on the lower beam should fail first since these bolts support the largest part of the panel's dead weight. However, the observed specific location of the failed bolts differs for all tests (Table 1). This might be explained by a scatter in the material properties of the bolts or by the attendance of less or more friction between the bolt shaft and the nut. For test numbers 2-2 and 4-1 rather brittle failure behaviour was observed while for the remaining tests a small decrease of the load was observed after the ultimate load was reached, preceding the final failure point. All failure modes were accompanied by a loud bang and at the same time a drop in load. After this load drop, it could be observed that the structure was still able to support some lateral load, since the load started to increase again. However, at that moment it was decided to end the tests as the structure was considered failed.

For test 5-1 failure occurred at the two tension corners of the panel (Fig. 10) with concrete spalling and reinforcement yielding. As no obvious load drop was observed, it was decided to end the test after a

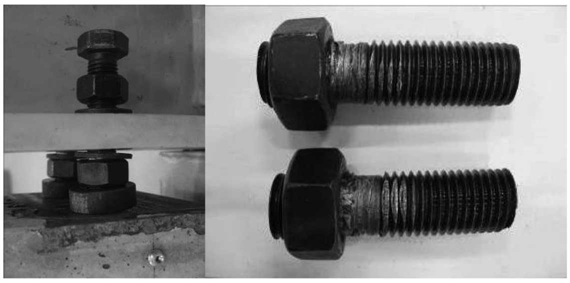

Fig. 9 'Bolt shear through nut' failure

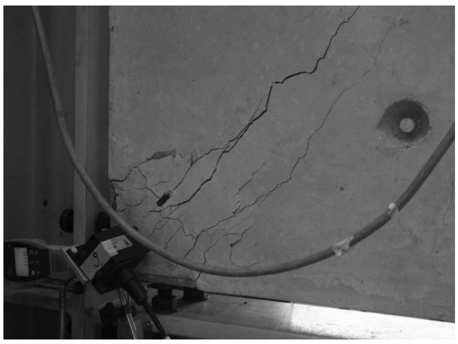

Fig. 10 Failure at panel corner with spalling and reinforcement yielding

lateral deflection was measured of 60 mm which is 1/50 times the height of the structure. At this moment the structure was still able to support a lateral load of 600 kN. Due to the substantial damage to the panel, a second test was not possible without making repairs. Therefore, test 5-2 was carried out using a repaired panel. In order to repair the panel, loose pieces of concrete were removed from the panel. Thereafter, the remaining holes were filled up with non-shrinking mortar. As a result of this repair, both the stiffness and ultimate strength of the structure decreased substantially, as can be seen in Fig. 8. Again, the structure failed at the tension corners of the panel.

On the basis of the load-deflection graphs, the stiffness and strength of all tested infilled frame structures can be quantified (Table 1). Terms used to describe the infilled frame behaviour are the ultimate strength (F_u), being the maximum load level reached, the secant stiffnesses ($k_{sec;1;if}$ and $k_{sec;2;if}$) and the tangent stiffness ($k_{tan;if}$) (Fig. 11). The secant stiffness $k_{sec;2;if}$ is determined by taking the ultimate load F_u with corresponding deflection. For secant stiffness $k_{sec;1;if}$ the load corresponding to a lateral deflection of 10 mm is taken, which is 1/300 of the height of the structure. The value 1/300 of the height of the structure is the recommended serviceability limit state for the lateral deflection of a storey in a multi-storey building according to Eurocode 3. The tangent stiffness is also determined at the lateral deflection of 10 mm, by calculating a linear regression over the range of 10 mm ± 1 mm. Finally, a comparison is made between the tangent stiffness of the infilled frame and its bare frame by means of a stiffness factor $\alpha = k_{tan;if} / k_{tan;bf}$.

The results in Table 1 show that the observed lateral stiffness of the infilled frames ranges between 4.0 and 13.3 times the bare frame stiffness, depending on the size of the window opening. Besides, all specimen types were able to support a lateral load of 583 kN or more. As mentioned before, for four panel geometries (type 1 to 4), the discrete connections were governing the strength of the structure as aimed at by design while for the test with the largest opening (type 5) the infill panel failed first.

5. Finite element modelling

The previous experimental research was supplemented by finite element analyses. The finite element package used was DIANA, release 9.2 (DIANA 2005). The aim of the finite element research is to develop and validate a finite element model that simulates the experimental infilled frame behaviour, taking into account non-linear material characteristics and geometrical non-linearity. The validated

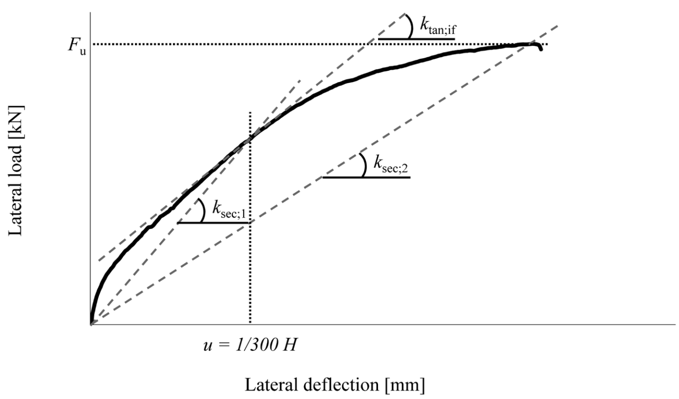

Fig. 11 Illustration of terms for consideration of infilled frame behaviour

finite element model can then be used to carry out parametric studies to investigate other configurations of the hybrid infilled frame.

5.1 Model design

A two-dimensional finite element model was created (Fig. 12). The model can be divided into three groups: panel, frame and discrete steel-concrete connections. For each group, the applied element types and material properties are discussed below.

5.1.1 Panel

The concrete panel is modelled with eight-node isoparametric plane stress elements CQ16M (DIANA 2005) with a thickness of 200 mm. The longitudinal reinforcement and stirrups are modelled with reinforcement bars, embedded in the plane stress elements. The technique of embedding allows the lines of the reinforcement to deviate from the lines of the mesh. The embedded reinforcements do not have degrees of freedom of their own. The reinforcement strains are computed from the displacement field of the plane stress elements, implying a perfect bond between the reinforcement and the surrounding concrete.

5.1.2 Frame

The three-node, two-dimensional class-III beam element CL9BE (DIANA 2005) is used to model the frame members. These elements are based on the so-called Mindlin–Reissner theory which takes shear deformation into account. The sectional properties of the beam elements correspond to the sections used experimentally (HE180M). The beam-to-column connection is modelled by a rigid offset to take the column depth into account, and a two-node rotational spring element SP2RO, (DIANA 2005) representing the stiffness of this connection.

5.1.3 Discrete steel-concrete connection

The discrete steel-concrete connections are represented by two-node translational spring elements SP2TR, (DIANA 2005), and are only able to support axial compressive forces. An initial force in the

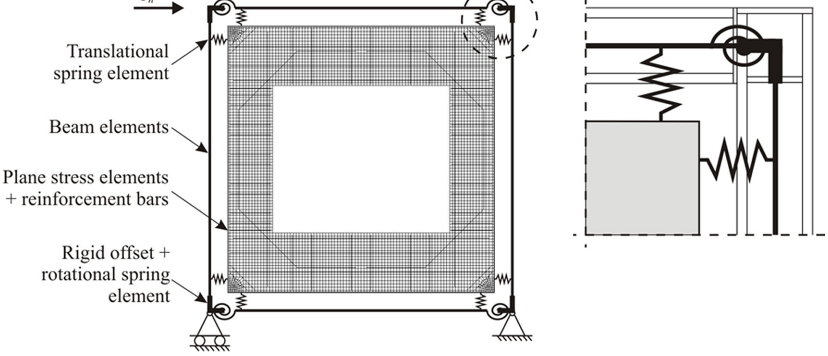

Fig. 12 Finite element model (specimen 3) with corner detail

springs is applied of 100 kN, representing the pretension resulting from the torque controlled tightening of the bolts. The magnitude of this prestress load was experimentally found.

5.2 Material properties

5.2.1 Panel

Prior to cracking, concrete can be modelled sufficiently accurately as isotropic, linear elastic (Borst 2002). The initial Young's modulus E_c was determined by performing standard material tests with concrete prisms, and can be found in Table 2. The Poisson's ratio of concrete under uni-axial compressive stress ranges from about 0.15 to 0.22, with a representative value of 0.19 or 0.20 (ASCE 1982). For this study, a Poisson's ratio was adopted of $\nu = 0.2$. Standard material tests were performed with concrete 150 mm cubes to find the actual tensile strength f_{ct} and compressive strength f_c (Table 2). A non-linear concrete material model was used that combines the Drucker-Prager plasticity model for the compressive regime with a smeared cracking model for the tensile regime. For the behaviour of the concrete in compression the Drucker-Prager yield surface limits the elastic state of stress. The DIANA software evaluates the yield surface using the current state of stress, the angle of internal friction ϕ and the cohesion c. According to recommendation by the DIANA software manual (DIANA 2005), the angle of internal fiction of the concrete can be approximated to be $\phi = 10^{o}$. The cohesion c can then be calculated as follows:

$$c = f_c(1 - sin\,\phi)/2\,cos\,\phi \tag{1}$$

For the smeared crack approach, a multi-directional fixed crack model is applied, in which typically the direction of the normal to the crack is fixed upon initiation of the crack. A linear stress cut-off criterion is applied, which means that a crack arises if the major principal tensile stress exceeds the minimum of f_{ct} and $f_{ct}\,(1 + \sigma_{lateral}\,/\,f_c)$, with $\sigma_{lateral}$ being the lateral principal stress. Besides, a linear tension softening based on fracture energy G_f is adopted according to the CEB-FIP Model Code (CEB-FIB Model Code 1990), adapted proportionally to the ratio between the nominal and the measured tensile strength (for G_f, see Table 2). The Mode-I fracture energy is released in an element if the tensile strength is exceeded and the deformations localize in the element. With this approach the results obtained with the analysis are objective with regard to mesh refinement. Due to cracking of concrete, the shear stiffness is reduced, generally known as shear retention. A constant shear retention factor $\beta =$ 0.2 is used which is a commonly adopted value (Borst 2002). For the embedded reinforcement bars, a Young's modulus of $E_s = 2.0E + 05$ N/mm^2 is assumed. The stress-strain curve of the reinforcement bars is assumed to be elastic-perfectly plastic, with yielding according to the Von-Mises criterion, with yield stress $\sigma_y =$ 560 N/mm^2.

Table 2 Material properties concrete

Test	E_c [N/mm^2]	f_c [N/mm^2]	f_{ct} [N/mm^2]	G_f [Nm/m^2]
1	3.54E+04	62.2	3.9	97
2	3.67E+04	64.4	3.9	99
3	3.66E+04	70.6	4.2	104
4	3.70E+04	75.6	4.4	109
5	3.72E+04	66.0	3.9	97

5.2.2 Frame

For the frame, steel having the elastic material properties Young's modulus $E_s = 2.1\mathrm{E} + 05$ N/mm^2 and Poisson's ratio $\nu = 0.3$ was used, in combination with Von Mises plasticity ($\sigma_y = 235$ N/mm^2). The rotation springs representing the beam-to-column connections were calibrated on the results of the full-scale experiments with the bare frames. A typical moment-rotation curve for the rotation springs is shown in Fig. 13.

5.2.3 Discrete steel-concrete connection

The discrete steel-concrete connections were modelled with non-linear translational spring elements, with no tension capacity. Input is a stiffness diagram (Fig. 14) which was obtained from preceding investigations into the structural behaviour of the steel-concrete connection (Teeuwen, *et al*. 2007).

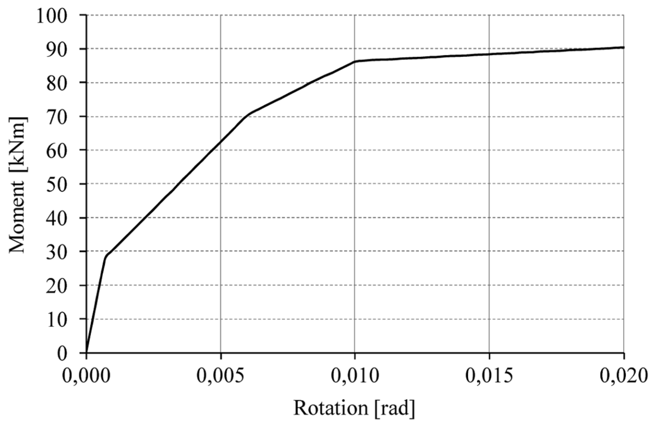

Fig. 13 Typical moment-rotation curve for rotation springs shown in Fig. 12

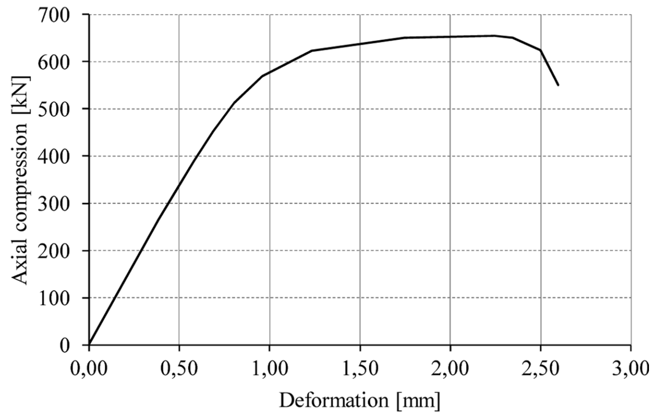

Fig. 14 Load-deformation curve for translation springs shown in Fig. 12

5.3 Boundary conditions and loading

Support conditions matching the test-setup were used. The loads applied to the finite element model include initial prestressing of the translation springs, representing the tightening of the steel-concrete connection (load case 1), the dead weight (load case 2), and horizontal loading at the left upper corner up to failure (load case 3). In the finite element analyses, the prestressing force from the bolts are simulated with initial stresses and applied to the infilled frame first. After the structure has become in an equilibrium condition, the dead weight is applied to the infilled frame. This order of loading is correct, since the bare frame was fixed to the horizontally positioned panel. Therefore, the dead weight initially did not influence the prestressing forces in the bolts. Finally, the lateral load is applied to the left upper corner of the infilled frame. A displacement controlled procedure was applied to impose the load up to failure, using the regular Newton-Raphson iteration procedure to find the solution. A phased analysis that comprises two calculation phases was conducted, to enable determining the effect of the prestressing and erecting of the specimen. Between the two phases, the finite element model changes by addition of the constraint in the left upper corner, which is needed to apply the lateral displacement to the model. The results from the first phase were automatically used as initial values in the second phase.

6. Validation finite element model

Validation of the finite element model was accomplished by comparing the following experimental and numerical results: the global load-deflection behaviour, the ultimate load with corresponding failure mode, the local panel and connection deformations and the final crack patterns. The results from specimen 3 have been selected for a more detailed discussion.

To explicitly treat the structural behaviour of the infilled frame at the different stages of loading, the deformed shapes of specimen 3 are shown (Fig. 15), presenting the deformation after the prestress load from the bolts and the dead weight only are applied to the model ($\delta_H = 0$) (left) and at ultimate deflection $\delta_H = \delta_u$ (right). As a result of the tightening of the bolts, the infill panel is slightly uniformly-prestressed in the steel frame. The magnitude of the prestress loads is initially equal in all springs. After

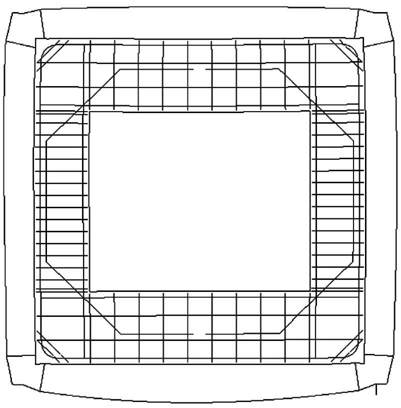

$\delta_H = 0$ (scale factor 1000)

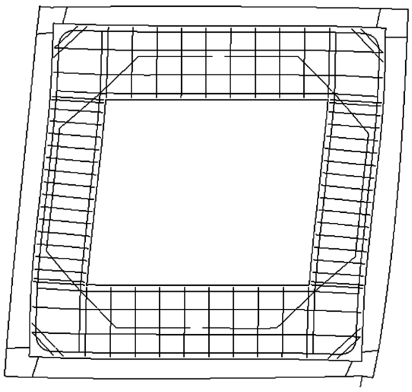

$\delta_H = \delta_u$ (scale factor 10)

Fig. 15 Deformed finite element model of specimen type 3 the dead load is applied to the model, the vertical springs at the bottom of the model are further loaded while the upper vertical springs are slightly unloaded. Thereafter, the horizontal load is applied to the model resulting in gradually unloading of the springs in the unloaded corners of the infilled frame. Although the translation springs in the unloaded corners are still in contact with the panel at ultimate deflection, they are unstressed since they are unable to support axial tensile forces. This is correct, as loss of contact between infill panel and frame in the tension corners was observed during the tests. From these figures we can observe that under lateral load, the infill panel tends to act as a diagonal strut bracing the steel frame. However, due to the presence of the opening in the panel, direct support from the load to the support by a strut under compression is impossible. Therefore the load is transferred around the opening to the support mainly by bending of the panel members, which is confirmed by the deformed shape of the panel.

The simulated and experimental global responses (test numbers n-1) of all specimens are presented in Fig. 16. Comparison shows that the load-deflection behaviour obtained from the FE-analysis is quite similar to the experimental results. The initial higher stiffness is present, followed by the approximately linear branch and finally failure. The simulated failure modes of specimens 1 to 4 are connection failure, which are identical to the experimental failure. However, contrary to the experimentally found locations of failure (for locations, see Table 1), the specific failure locations for all simulations are identical, being the vertical translation spring in the right lower corner. Theoretically this is correct, since this translation spring is, besides the lateral load, also loaded with a major part of the dead weight of the infill panel. However, there is only a slight difference with the magnitude of the axial forces in the other loaded springs at ultimate load ($\pm 2.5\%$), and other phenomena such as the exact magnitude of the prestress load and the level of friction in the connections are also contributory to the experimental location of failure. Therefore, the experimentally found failure locations in some tests differ from the simulated ones.

For test 5 the infill panel failed first with considerable deformations concentrated in open cracks and yielding of the wedge reinforcement. Although the finite element simulation indicates panel failure with yielding of the wedge reinforcement, the smeared crack model is not appropriate to adequately describe the post-peak behaviour. To obtain a more accurate post-peak prediction, the concrete model could be supplied with discrete cracks. In this combined approach, the smeared crack model is used to model the distributed cracking and concrete crushing, while interface elements are inserted between the continuum elements along the potential crack path, where major cracking can be expected based on the

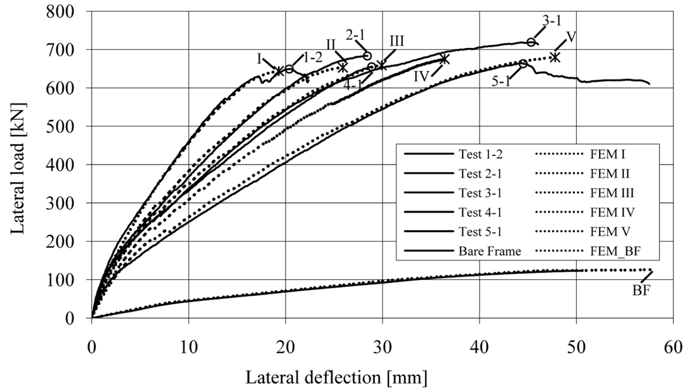

Fig. 16 Simulated and experimental load deflection response of infilled frames

experimental observations. However, panel failure will be prevented in the design since the steel-concrete connection will be designed to govern the strength of the structure. Therefore, the smeared crack approach is satisfactory for design purposes.

Besides the global behaviour, also the accuracy of the simulated local behaviour of the infill panel was investigated. Six LVDTs (Fig. 6: δa to δf) were positioned on the concrete panel surface, measuring local deformations over a distance of 300 mm in order to determine average strains and crack initiation in the tension zones of the panel. For each LVDT measurement, a comparison was made between the experiment and the simulation. In Fig. 17 the measured and simulated average strains for test 3 are presented (LDVTs δc, δd and δe). It is shown that the FE model qualitatively represents the strains on the surface of the concrete panel reasonably accurate and thus, also by this check, the FE model may be considered to be validated. Also for the other simulations, sufficient agreement was shown between the measured and simulated local panel deformations.

To provide a better understanding of the stress distribution in the infill panel, the deformed shape of the panel of specimen 3, together with a contour plot of the major principal stresses at ultimate load is shown in Fig. 18. The figure shows that the two window corners loaded in compression are subjected to large compressive stresses. Concrete crushing is indicated in the elements surrounding these window

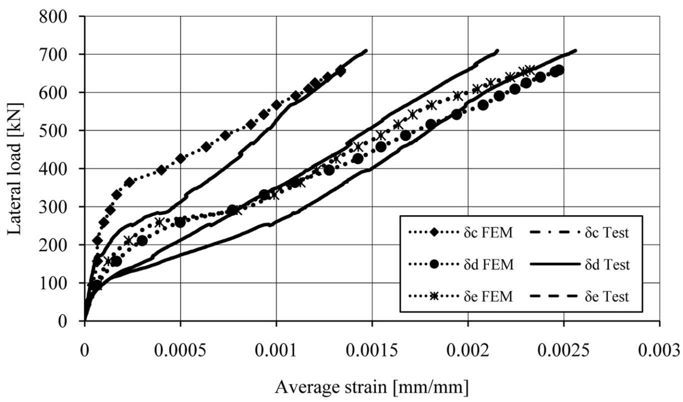

Fig. 17 Measured and simulated strains for specimen 3

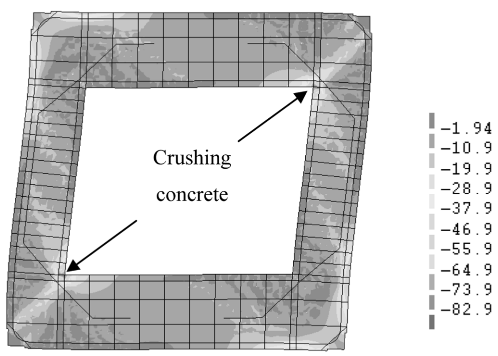

Fig. 18 Deformed panel with minor (compressive) principal stresses (specimen 3 at ultimate load)

corners when considering the Von Mises plastic strains. This phenomenon was not observed during the experiments but is shown in all simulated tests. Confirmed by the fact that in none of the simulations the crushed area expands to other elements than the ones directly surrounding the window corner, the high plastic strains may be attributed to the geometrical discontinuity (right angle) that is present at the window corners.

In Fig. 19 the smeared crack patterns of the concrete panels at ultimate load are presented, together with the experimentally found crack patterns after the panel's first test. Considering the experimental crack patterns it can be noticed that the patterns are qualitatively identical while the crack intensity increases when the window opening becomes larger. Only for the last test, considerable large crack widths were observed in some regions of the panel. Comparing the experimental crack patterns with the simulated ones, good qualitative agreement between the numerical crack patterns and the experimental crack patterns is observed.

The comparisons presented above between experimental observations and numerical predictions of the hybrid lateral load resisting infilled frame indicate that the finite element model used in this study is adequate, and that the corresponding results are reliable. The finite element investigation will, therefore, be further extended to investigate other configurations of hybrid lateral load resisting infilled frames in a parameter study that serves as a basis for the development of design rules.

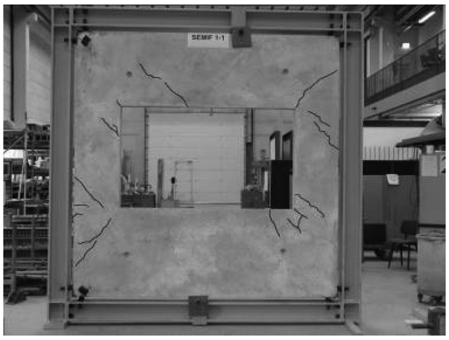

Test 1-1

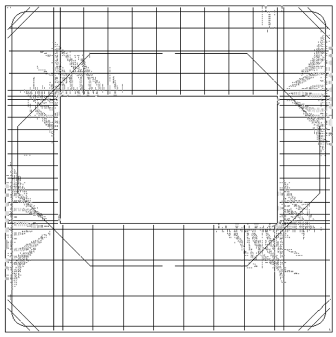

FEM I

(a) Specimen type 1

Test 2-1

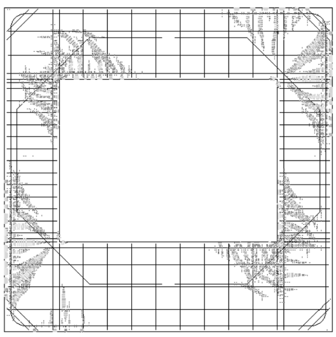

FEM II

(b) Specimen type 2

Fig. 19 Experimental and simulated final crack patterns

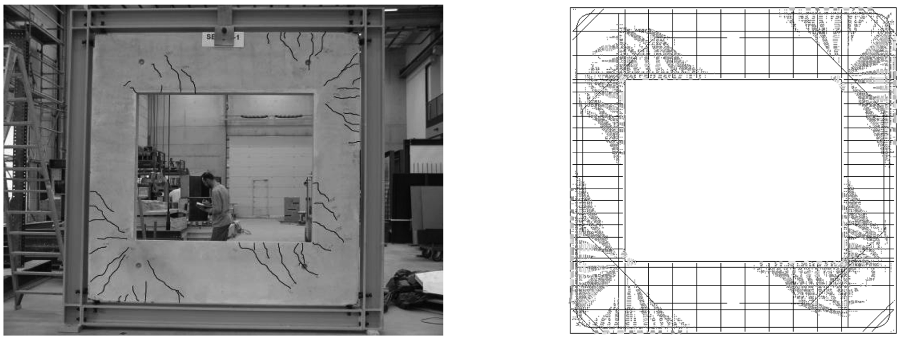

Test 3-1 FEM III

(c) Specimen type 3

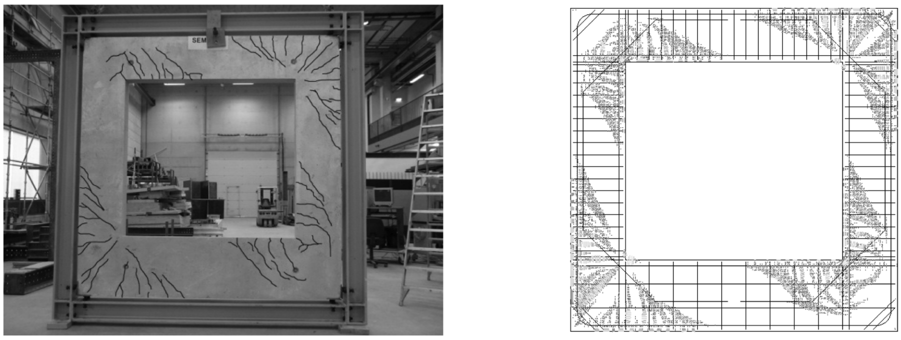

Test 4-1 FEM IV

(d) Specimen type 4

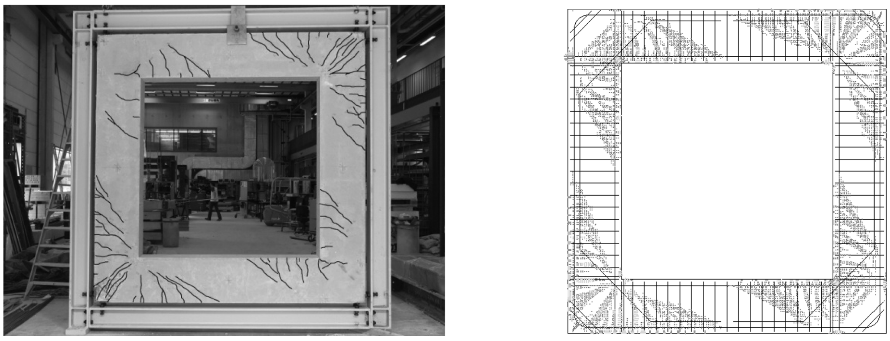

Test 5-1 FEM V

(e) Specimen type 5

Fig. 19 Continued.

7. Conclusions

In this study, the behaviour of infilled steel frames with discretely connected precast concrete panels provided with a window opening was investigated. One-storey, one-bay infilled frames were subjected to experimental and numerical analyses. Based on the results, the following conclusions can be drawn:

The experiments show that discretely connected precast concrete panels with window openings can significantly improve the performance of steel frames. The observed tangent stiffnesses at a deflection of 1/300 of the height of the structure range between 4 and 13 times the bare frame stiffness, depending on the size of window opening. The ultimate strength of the infilled frames ranges from 583 to 719 kN. For four panel geometries, the strength of the structures was governed by the discrete connections as aimed for by design, while for the test with the largest window opening the infill panel failed first.

Finite element simulations were performed taking into account non-linear material properties and geometrical non-linearity. A comparison between the full-scale experiments and simulations shows that the FE model presented in this paper is able to predict the lateral load versus deflection relationship of the hybrid lateral load resisting infilled frame, and the ultimate lateral load carrying capacity for all failure mechanisms. Therefore, the FE-study will be extended to study the infilled frame performance by varying different parameters. Based on this parameter study, design rules for infilled steel frames with discretely connected precast concrete panels will be developed.

References

ASCE task committee on concrete and masonry structure (1982), *State of the art report on Finite Element Analysis of Reinforced Concrete*, ASCE, New York.

Borst, R. (2002), "Fracture in Quasi-brittle Materials: a review of Continuum Damage-based approaches", *Eng. Fract. Mech.*, **69**, 95-112.

CEB Comite Euro International Du Beton (1993), *CEB-FIP Model Code 1990: design code*, Thomas Telford, London.

Diana (2005), *Diana user's manual release 9*, TNO Diana bv, Delft, the Netherlands.

Hoenderkamp, J.C.D., Hofmeyer, H. and Snijder, H.H. (2005), "Composite behaviour of steel frames with precast concrete infill panels", In Hoffmeister, B. and Hechler, O. (Eds.) *Proc. of the 4th European conf. on steel & composite structures*, Druck &Verlagshaus Mainz GmbH, Aachen.

Holmes, M. (1961), "Steel frames with brickwork and concrete infilling", *Proc. Inst. Civ. Eng.,* **19**, 473-478.

Liauw, T.C. (1972), "An approximate method of analyses for infilled frames with or without opening", *Build. Sci.*, **7**, 233-238.

Liauw, T.C. and Kwan, K.H. (1983), "Plastic theory of non-integral infilled frames", *Proc. Inst. Civ. Eng*, Part 2, **75**, 379-396.

Mainstone, R.J. (1971), "On the stiffnesses and strengths of infilled frames", *Proc. Inst. Civ. Eng,* Supplement IV, Paper 7360S, 57-90.

Mallick, D.V. and Garg, R.P. (1971), "Effect of openings on the lateral stiffness of infilled frames", *Proc. Inst. Civ. Eng.*, **49**, 193-210.

Mallick, D.V. and Severn, R.T. (1967), "The behaviour of infilled frames under static loading", *Proc. Inst. Civ. Eng.,* **38**, 639-656.

Muttoni, A., Schwartz, J. and Thurlimann, B. (1997), *Design of Concrete Structures with Stress Fields*, Birkhauser, Berlin.

Ng'andu, B.M. (2006), *Bracing steel frames with calcium silicate element walls*, PhD-thesis, Eindhoven University of Technology, Eindhoven, the Netherlands.

Polyakov, S.V. (1957), "On the interaction between masonry filler walls and enclosing frame when loaded in the plane of the wall", *Construction in seismic regions*, Moscow, Translation in *Earthquake Engineering,* Earthquake Engineering Research Institute, San Francisco, 1960, 36-42.

Stafford Smith, B. (1962), "Lateral stiffness of infilled frames", *J. Struct. Div.*, ASCE, **88**(ST6), 183-199.

Stafford Smith, B. (1966), "Behaviour of square infilled frames", *J. Struct. Div.*, ASCE, **92**(ST1), 381-403.

Tang, R.B., Hoenderkamp, J.C.D. and Snijder, H.H. (2000), "Preliminary numerical research on steel frames with precast reinforced concrete infill panels", In Yang, Y.B., Leu, L.J. and Hsieh, S.H. (Eds.), *Proc. of the 1st Int. Conf. on Structural Stability and Dynamics*, Taipei.

Teeuwen, P.A., Kleinman, C.S., Snijder, H.H. and Hofmeyer, H. (2007), "Experiments and FE-model for a connection between steel frames and precast concrete infill panels", In Eligehausen, R., Fuchs, W., Genesio, G.

and Grosser, P. (Eds.), *Proc. of the 2nd Int. Symp. on Connections between Steel and Concrete*, Ibidem-Verlag, Stuttgart.

Teeuwen, P.A., Kleinman, C.S., Snijder, H.H. and Hofmeyer, H. (2008a), “Analysis of steel frames with precast concrete infill panels”, In IABSE-AIPPC-IVBH (Ed.), *Proc. of the 17th Congress of IABSE, Creating and Renewing Urban Structures- Tall Buildings, Bridges and Infrastructure*, Chicago.

Teeuwen, P.A., Kleinman, C.S., Snijder, H.H. and Hofmeyer, H. (2008b), “Full-scale testing of infilled steel frames with precast concrete panels provided with a window opening”, *Heron,* **53**(4), 195-224 (available online at http://heron.tudelft.nl).

Wood, R.H. (1978), “Plasticity, composite action and collapse design of unreinforced shear wall panels in frames”, *Proc. Inst. Civ. Eng.*, Part 2, **65**, 381-411.

DN